

Tautomeric and Conformational Properties of Malonamic Acid Methyl Ester, $\text{NH}_2\text{C}(\text{O})\text{-CH}_2\text{-C}(\text{O})\text{OCH}_3$: Electron Diffraction and Quantum Chemical Study

Natalya V. Belova,^{*,†} Heinz Oberhammer,[‡] and Sergey A. Shlykov[†]

Ivanovo State University of Chemistry and Technology, 153460 Ivanovo, Russia, and Institut für Physikalische und Theoretische Chemie, Universität Tübingen, 72076 Tübingen, Germany

Received: December 3, 2007; In Final Form: January 21, 2008

The tautomeric and conformational properties of malonamic acid methyl ester, $\text{NH}_2\text{C}(\text{O})\text{-CH}_2\text{-C}(\text{O})\text{OCH}_3$, have been investigated by means of gas-phase electron diffraction (GED) and quantum chemical calculations (HF, B3LYP, and MP2 approximations with different basis sets up to 6-311++G(3df,pd)). Both quantum chemistry and GED at 360(8) K result in the existence of a single diketo conformer in the gas phase. According to GED refinement, this conformer possesses an (ac, sc) conformation with dihedral angles $\text{C-C-C}(\text{NH}_2)=\text{O}$ of $140.3(3.0)^\circ$ and $\text{C-C-C}(\text{OCH}_3)=\text{O}$ of $31.1(7.2)^\circ$. The experimental geometric parameters are reproduced very closely by MP2 and B3LYP methods with large basis sets.

Introduction

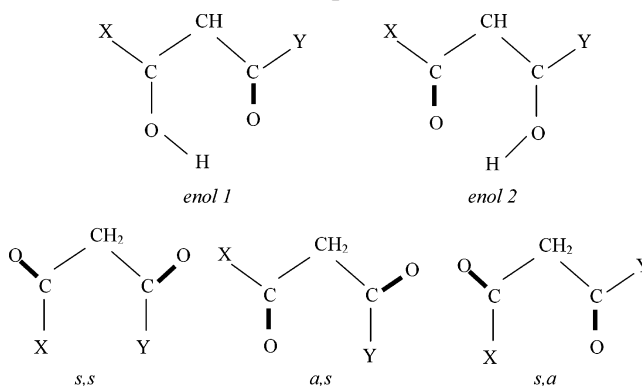
Tautomeric and conformational properties of β -dicarbonyl compounds (β -diketones) of the type $\text{XC}(\text{O})\text{-CH}_2\text{-C}(\text{O})\text{Y}$ (see Scheme 1) continue to attract great interest for many years.¹ In such compounds, two enol forms can occur, with the O–H bond adjacent to X or to Y (see Scheme 1). For the diketo tautomer, different conformations are feasible, depending on the relative orientations of the two $\text{C}=\text{O}$ bonds (Scheme 1, “s” stands for synperiplanar (sp) or synclinal (sc) and “a” for antiperiplanar (ap) or anticlinal (ac)²).

It has been observed that both tautomeric and conformational properties depend strongly on the substituents X and Y, but very little is known about the correlation of these properties and the nature of the substituents. In previous studies,^{3,4} we have formulated the rule that substituents of group I (H, CH_3 , $\text{C}(\text{CH}_3)_3$, or CF_3) favor the enol tautomer, whereas substituents of group II (F, Cl, NH_2 , or OCH_3) favor the diketo form. Thus, according to gas-phase structural studies, the enol tautomer is strongly preferred for $\text{X} = \text{Y} = \text{H}$,^{5–7} CH_3 ,^{8–11} $\text{C}(\text{CH}_3)_3$,¹² and CF_3 .¹³ On the other hand, compounds with $\text{X} = \text{Y} = \text{F}$,¹⁴ Cl,¹⁵ OCH_3 ,¹⁶ or NH_2 ⁴ exist in the diketo form only.

In previous investigations, we have studied the tautomeric and conformational properties of two dicarbonyl compounds which contain substituents belonging to different groups (I and II): methyl acetoacetate, $\text{CH}_3\text{C}(\text{O})\text{-CH}_2\text{-C}(\text{O})\text{OCH}_3$ ($\text{X} = \text{CH}_3$ and $\text{Y} = \text{OCH}_3$)¹⁷ and acetoacetamide, $\text{CH}_3\text{C}(\text{O})\text{-CH}_2\text{-C}(\text{O})\text{-NH}_2$ ($\text{X} = \text{CH}_3$ and $\text{Y} = \text{NH}_2$).³ In these compounds, the CH_3 group favors the enol tautomer, whereas OCH_3 and NH_2 groups favor the diketo form. In both cases, GED studies resulted in mixtures of both tautomers, 80(7)% enol and 20(7)% diketo in methyl acetoacetate and 63(7)% enol and 37(7)% diketo in acetoacetamide.

In the present study, we report a gas electron diffraction (GED) investigation combined with quantum chemical calculations for malonamic acid methyl ester, $\text{NH}_2\text{C}(\text{O})\text{-CH}_2\text{-C}(\text{O})\text{-OCH}_3$, (MAME), which also contains different substituents, X

SCHEME 1: Two Possible Enol Tautomers (Top) and Three Possible Conformers of Diketo Tautomer (Bottom) of $\text{XC}(\text{O})\text{-CH}_2\text{-C}(\text{O})\text{Y}$ Compounds



$= \text{NH}_2$ and $\text{Y} = \text{OCH}_3$. In this case, however, both substituents belong to group II. Therefore, we expect the diketo tautomer to be strongly predominant in this dicarbonyl compound. As pointed out in Scheme 1, different keto conformers of MAME can exist. Previous GED studies for β -diketones with equal substituents $\text{X} = \text{Y}$ resulted in different conformational properties. In dimethyl malonate, $\text{CH}_3\text{OC}(\text{O})\text{-CH}_2\text{-C}(\text{O})\text{OCH}_3$ (DMM), with $\text{X} = \text{Y} = \text{OCH}_3$, a mixture of two diketo conformers is present, 69(10)% (ac, ac) conformer with C_2 symmetry and 31(10)% (ac, sp) conformer with C_1 symmetry.¹⁶ On the other hand, a GED study of malonamide, $\text{NH}_2\text{C}(\text{O})\text{-CH}_2\text{-C}(\text{O})\text{NH}_2$ (MA), with $\text{X} = \text{Y} = \text{NH}_2$ resulted in the presence of a single (ac, sc) conformer with a weak intramolecular $\text{N-H}\cdots\text{O}$ hydrogen bond.⁴ In this context, the number of stable conformers of MAME is of great interest. So far, no information about tautomeric, conformational, or structural properties of this compound has been reported in the literature.

Quantum Chemical Calculations

All quantum chemical calculations were performed with the program set Gaussian 03.¹⁸ To detect all possible diketo conformers, a two-dimensional potential energy surface has been scanned with the B3LYP/6-31G(d,p) method. The torsional

* Corresponding author.

[†] Ivanovo State University of Chemistry and Technology.

[‡] Universität Tübingen.

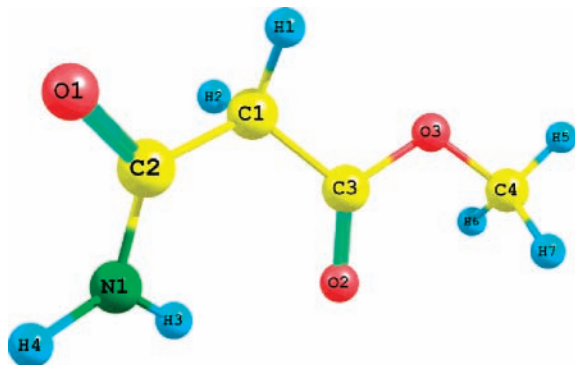


Figure 1. Molecular structure of malonamic acid methyl ester.

angles $\tau(\text{C3C1C2O1})$ and $\tau(\text{C2C1C3O2})$ were changed in steps of 20° with full optimization of all other parameters. (See Figure 1 for atom numbering.) The potential surface (Figure 2) possesses a single deep minimum for (ac, sc) conformer with

$\tau(\text{C3C1C2O1})$ about 140° and $\tau(\text{C2C1C3O2})$ about 40° . The geometries of the enol and diketo tautomer of the malonamic acid methyl ester (MAME) were optimized with the HF approximation (3-21G basis set), and with MP2 and B3LYP methods (6-31G(d,p) basis sets). Two possible enol conformers (see Scheme 1) were taken into account. The relative energies ($\Delta E = E_{\text{keto}} - E_{\text{enol}}$) and relative free energies ($\Delta G^0 = G_{\text{keto}}^0 - G_{\text{enol}}^0$) obtained with the different computational methods are summarized in Table 1.

According to these predictions, the two stable enol forms possess much higher energies than the diketo form. The predicted Gibbs free energy differences vary from 3.4 to 12.1 kcal/mol and from 11.0 to 17.8 kcal/mol for enol1 and enol2, respectively. Thus, all methods predict a strong preference of the diketo form. The geometry of this diketo tautomer of MAME was furthermore fully optimized with the MP2 and B3LYP methods and 6-311++G(3df,pd) basis sets. The geometric parameters derived with these methods are listed in Table 2,

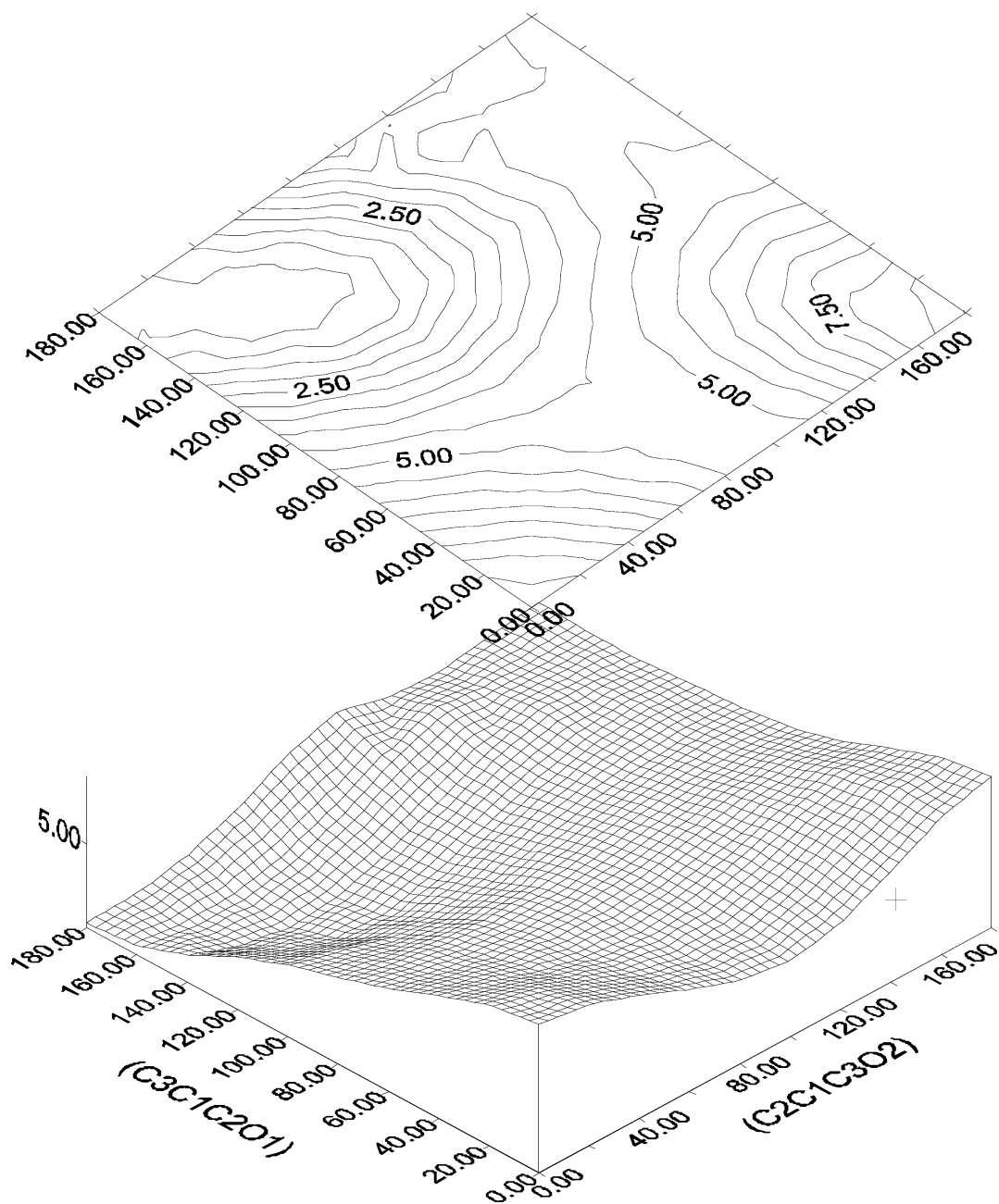


Figure 2. Potential energy surface for malonamic acid methyl ester obtained by rotation around C–C bonds.

TABLE 1: Optimized Relative Energies and Gibbs Free Energies of the Enol Tautomers and Diketo Conformer of Malonic Acid Methyl Ester

	keto	enol 1 ^a	enol 2 ^a
HF/3-21G			
E_{rel} , kcal/mol	0.0	1.70	9.00
G_{rel}^0 , kcal/mol	0.0	3.43	11.00
MP2/6-31G(d,p)			
E_{rel} , kcal/mol	0.0	11.17	16.81
G_{rel}^0 , kcal/mol	0.0	12.09	17.76
B3LYP/6-31G(d,p)			
E_{rel} , kcal/mol	0.0	6.41	11.56
G_{rel}^0 , kcal/mol	0.0	7.67	12.76

^a Enol 1: O–H bond is adjacent to the NH₂ group, NH₂C(OH)=CH–C(O)OCH₃. Enol 2: O–H bond is adjacent to methoxy group, NH₂C(O)–CH=C(OH)OCH₃

TABLE 2: Experimental and Calculated Geometric Parameters of the Diketo Tautomer of Malonic Acid Methyl Ester^a

parameters	GED (r_{hl} , α_{hl}) ^b	B3LYP/	MP2/
		6-311++G- (3df,pd)	6-311++G- (3df,pd)
r(C1–C2)	1.530(4)	1.535	1.528
r(C1–C3)	1.505(4) ^c	1.511	1.505
r(C2–O1)	1.222(3)	1.215	1.219
r(C3–O2)	1.216(3) ^c	1.210	1.215
r(C3–O3)	1.344(3) ^c	1.338	1.337
r(O3–C4)	1.446(3) ^c	1.439	1.436
r(C2–N)	1.360(4)	1.352	1.354
r(N–H3)	1.011(4)	1.011	1.011
r(N–H4)	1.008(4) ^c	1.007	1.008
r(C1–H1)	1.087(4) ^c	1.086	1.086
r(C1–H2)	1.096(4) ^c	1.096	1.095
r(C4–H5)	1.086(4) ^c	1.086	1.085
r(C4–H6)	1.090(4) ^c	1.089	1.089
r(C4–H7)	1.089(4) ^c	1.089	1.089
∠C2C1C3	116.4(1.4)	117.8	115.4
∠C1C2O1	119.2(1.1)	119.5	120.5
∠C1C3O2	125.3(1.1)	125.6	125.2
∠C1C2N	116.3(1.3)	116.5	115.5
∠C1C3O3	111.2(1.3)	111.2	111.5
∠C3O3C4	115.6(1.0)	116.3	114.7
∠H1C1C2	107.6 ^d	107.6	107.9
∠H1C1C3	110.6 ^d	110.6	111.0
∠H2C1C2	106.6 ^d	106.6	106.9
∠H2C1C3	106.6 ^d	106.6	106.8
∠H3NC2	120.3 ^d	120.3	119.9
∠H4NC2	117.9 ^d	117.9	117.6
∠H5C4O3	105.4 ^d	105.4	105.3
∠H6C4O3	110.4 ^d	110.4	110.2
∠H7C4O3	110.3 ^d	110.3	110.2
∠H6C4H5	110.7 ^d	110.7	110.9
∠H7C4H5	110.7 ^d	110.7	110.9
τ(C1C2NH3)	10.2 ^d	10.2	12.7
τ(O1C2NH4)	–4.5 ^d	–4.5	–6.3
τ(C3O3C4H5)	180.3 ^d	180.3	179.8
τ(NC2C1O1)	177.1(5.4)	177.1	176.8
τ(O3C3C1O2)	179.5(4.6)	178.7	179.1
τ(C4O3C3O2)	–0.4(9.6)	0.8	0.5
τ(C2C1C3O2)	31.1(7.2)	38.2	49.3
τ(C3C1C2O1)	140.3(3.0)	151.0	142.9

^a Distances in angstroms and angles in degrees. For atom numbering, see Figure 1. ^b Uncertainties in r_{hl} $\sigma = (\sigma_{\text{sc}}^2 + (2.5\sigma_{\text{LS}})^2)^{1/2}$ ($\sigma_{\text{sc}} = 0.002r$, σ_{LS} : standard deviation in least-squares refinement), for angles $\sigma = 3\sigma_{\text{LS}}$. ^c Difference to previous parameter fixed to calculated (B3LYP) value. ^d Not refined.

together with the experimental results. It should be noted that all geometric parameters optimized at different levels of theory are very close, except for the torsional angles $\tau(\text{C3C1C2O1})$ and $\tau(\text{C2C1C3O2})$. All calculations including electron correla-

TABLE 3: Interatomic Distances, Vibrational Amplitudes, and Vibrational Corrections for the Diketo Tautomer of Malonic Acid Methyl Ester (Excluding Nonbonded Distances Involving Hydrogen)^a

	r_{hl}^b	l(GED) ^b	l(B3LYP) ^c	$r_{\text{hl}} - r_{\text{a}}^c$
N–H4	1.008(4)	0.075(3) 11 ^d	0.069	0.0051
N–H3	1.011(4)	0.076(3) 11	0.069	0.0068
C4–H5	1.086(4)	0.082(3) 11	0.076	0.0013
C1–H1	1.087(4)	0.082(3) 11	0.076	0.0006
C4–H7	1.089(4)	0.083(3) 11	0.077	0.0014
C4–H6	1.090(4)	0.083(3) 11	0.077	0.0015
C1–H2	1.096(4)	0.084(3) 11	0.077	0.0020
C3–O2	1.216(3)	0.044(3) 11	0.038	0.0009
C2–O1	1.222(3)	0.044(3) 11	0.038	–0.0009
C3–O3	1.344(3)	0.052(3) 11	0.046	–0.0017
C2–N	1.360(4)	0.051(3) 11	0.045	0.0174
O3–C4	1.4446(4)	0.056(3) 11	0.050	0.0008
C1–C3	1.505(4)	0.058(3) 11	0.052	0.0021
C1–C2	1.530(4)	0.060(3) 11	0.054	–0.0017
O2···O3	2.256(6)	0.050(3) 12	0.052	0.0035
N···O1	2.285(6)	0.052(3) 12	0.054	0.0169
C1···O3	2.353(15)	0.064(3) 12	0.066	0.0019
C4···C3	2.362(8)	0.064(3) 12	0.066	0.0035
C1···O1	2.379(12)	0.063(3) 12	0.065	0.0103
C1···O2	2.421(12)	0.061(3) 12	0.063	0.0037
C1···N	2.456(14)	0.064(3) 12	0.066	0.0018
C2···C3	2.580(12)	0.081(3) 12	0.083	–0.0202
C4···O2	2.655(13)	0.099(3) 12	0.101	0.0076
O2···N	2.786(14)	0.164(8) 13	0.161	–0.0951
C3···N	2.955(10)	0.118(8) 13	0.115	0.0588
C2···O2	2.980(12)	0.112(8) 13	0.109	–0.1071
C3···O1	3.604(19)	0.076(4) 14	0.124	–0.0539
C2···O3	3.680(25)	0.120(4) 14	0.168	0.0735
C1···C4	3.694(14)	0.070(4) 15	0.071	0.0130
O1···O2	4.126(16)	0.132(12) 16	0.127	–0.1317
O3···N	4.263(21)	0.191(12) 16	0.186	0.2114
O1···O3	4.511(37)	0.271(12) 16	0.265	0.0251
C2···C4	4.887(33)	0.251(33) 17	0.179	0.0635
C4···N	5.219(27)	0.294(33) 17	0.223	0.2209
C4···O1	5.790(53)	0.238(51) 18	0.293	0.0069

^a Values in angstroms. Error limits for the amplitudes are 3σ values. For atom numbering, see Figure 1. ^b r_{hl} , l(GED): interatomic distances and vibrational amplitudes derived from GED data. ^c Derived from theoretical force field (B3LYP/6-311++G(3df,pd)) with the method of Sipachev, using the program SHRINK.¹⁹ ^d Group number of amplitude.

tion (MP2 and B3LYP) predict an (ac, sc) conformation with torsional angles between 136° and 151° for $\tau(\text{C3C1C2O1})$ and between 38° and 49° for $\tau(\text{C2C1C3O2})$. The HF approximation, however, results in an (ap, sp) conformation with dihedral angles of 180° and 0°. Comparison of the HF results for relative energies of the tautomers and the geometry of the diketo form with those derived with MP2 and B3LYP methods demonstrates that the HF method with small basis sets is inadequate for a molecule of this type. Also, the two methods which include electron correlation result in rather different relative energies of the enol tautomers. Both methods, however, predict the presence of the keto tautomer only.

Vibrational amplitudes and corrections, $\Delta r = r_{\text{hl}} - r_{\text{a}}$, were derived from a theoretical force field (B3LYP/6-311++G(3df,pd)) with the method of Sipachev, using the program SHRINK.¹⁹ The values of l and Δr are included in Table 3.

Structure Analysis

The experimental geometric structure MAME was determined with a combined GED/mass spectrometric method. The heaviest ion in the mass spectrum was the parent ion, [C₄H₇NO₃]⁺ (Table 5). This demonstrates that monomers are present in the vapor at the conditions of the simultaneous GED/MS experiment. No

TABLE 4: Conditions of GED/MS Experiment

nozzle-to-plate distance, mm	338	598
fast electrons beam, μA	1.06	0.42
accelerating voltage, kV	74.5	68.1
electron wavelength, \AA	0.04341(4)	0.04554(4)
temperature of effusion cell, K	365(5)	354(5)
ionization voltage, V	50	50
exposure time, s	110–120	50–55
residual gas pressure, Torr	3.3×10^{-6}	4.8×10^{-6}

TABLE 5: Mass Spectral Data of the Vapor of $\text{C}_4\text{H}_7\text{NO}_3^a$

ion ^b	<i>m/e</i> , amu	abundance, %
[OCH] ⁺	29	12
[OCH ₂] ⁺	30	11
[OCH ₃] ⁺	31	14
[C(O)CH] ⁺	41	7
[C(O)CH ₂] ⁺	42	47
[HNC(O)] ⁺ , [C(O)CH ₃] ⁺	43	100
[H ₂ NC(O)] ⁺	44	64
[H ₂ NC(O)CH] ⁺	57	5
[C(O)OCH ₃] ⁺	59	23
[C(O)CHC(O)] ⁺	69	8
[H ₂ CC(O)OCH ₃] ⁺	73	88
[M–NH ₂ –CH ₃] ⁺	86	17
[M] ⁺	117	15

^a Only peaks with abundance $\geq 5\%$. ^b M = $\text{C}_4\text{H}_7\text{NO}_3$.

ions were detected, which could arise from impurities. The experimental radial distribution function (Figure 3) was derived by Fourier transformation of the experimental intensities. Comparison with calculated radial distribution functions demonstrates that the experimental curve can be reproduced very well with a single diketo tautomer (see Figure 3).

In the least-squares analyses with a modified version of the program KCED²⁰ the differences between all C–H and N–H bond lengths, between all C–O, and between both C–C bond lengths were constrained to calculated values (B3LYP/6-311++G(3df,pd)). Furthermore, all angles which determine the positions of H atoms were fixed to calculated values. Preliminary geometric parameters from B3LYP/6-311++G(3df,pd) calculation were then refined by a least-squares procedure of the molecular intensities. Independent r_{H1} parameters were used to describe the molecular structure. In addition to four bond lengths, six bond angles and five dihedral angles (see Table 2) were refined. Vibrational amplitudes were refined in groups 11 to 18 with fixed differences within each group. Seven correlation coefficients had values larger than |0.7|: $\angle(\text{C1C2O1})/\tau(\text{C2C1C3O2}) = -0.73$, $\angle(\text{C1C2O1})/\angle(\text{C1C2N}) = -0.95$, $\tau(\text{N2C2O1})/\tau(\text{C3C1C2O1}) = -0.78$, $\angle(\text{C1C3O3})/\angle(\text{C1C2O1}) = -0.96$, $\angle(\text{C1C3O3})/\angle(\text{C1C2N}) = 0.88$, $\tau(\text{O3C3C1O2})/\angle(\text{C2C1C3}) = 0.71$, $\tau(\text{O3C3C1O2})/\tau(\text{C2C1C3O2}) = -0.88$.

The agreement factor for a single diketo conformer in the vapor at 87(8) °C was $R_f = 3.7\%$. ($R_f = 1.8\%$ and 5.3% for long and short nozzle-to-plate distances, respectively). Final results of the least-squares analysis are given in Table 2 (geometric parameters) and Table 3 (vibrational amplitudes). The refined geometrical parameters are rather similar to those predicted by the quantum chemical calculations. Only the torsion angles $\tau(\text{C3C1C2O1})$ and $\tau(\text{C2C1C3O2})$ differ by up to almost 20° from calculated values which depend strongly on the computational method, as pointed out above.

Discussion

The GED experiment for MAME, $\text{NH}_2\text{C}(\text{O})\text{--CH}_2\text{--C}(\text{O})\text{--OCH}_3$, which is a dicarbonyl compound with non-symmetric substituents, NH_2 and OCH_3 , results in the presence of a single

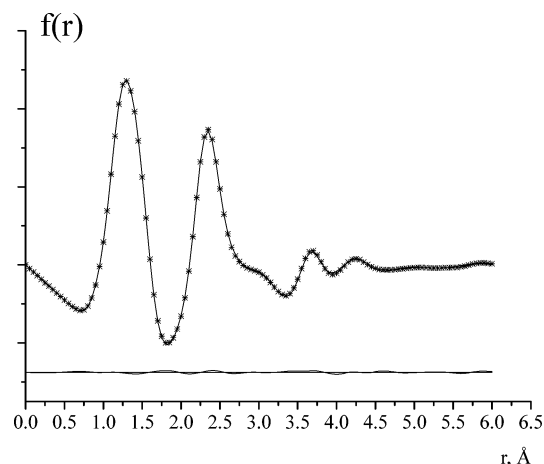


Figure 3. Experimental (dots) and calculated (solid line) radial distribution curves and the residuals (experimental–theoretical).

diketo conformer in the gas phase at 87(8) °C. This result is in agreement with the predictions by quantum chemical calculations. The presence of only the keto form extends the rule about tautomeric properties of dicarbonyl compounds which was formulated in the Introduction: β -diketones with equal substituents from group II (F, Cl, OCH_3 , NH_2) exist in the keto form. The result for MAME demonstrates that mixed substituents from group II also strongly favor the diketo tautomer.

Not only tautomeric but also conformational properties of keto tautomers depend on the substituents X and Y (see Scheme 1). The symmetrically substituted compounds with $X = Y = \text{F}$,¹⁴ Cl ,¹⁵ and OCH_3 ,¹⁶ exist as mixtures of two conformers with (ac, sp) and (ac, ac) orientations of the C=O bonds. In the case of $X = Y = \text{NH}_2$, only a single (ac, sc) conformer is present.⁴ Similarly, MAME with $X = \text{NH}_2$ and $Y = \text{OCH}_3$ and acetoacetamide, $\text{NH}_2\text{C}(\text{O})\text{--CH}_2\text{--C}(\text{O})\text{CH}_3$ (AAA), with $X = \text{NH}_2$ and $Y = \text{CH}_3$ possess only a single keto conformer in the gas phase. We suppose that in the presence of at least one NH_2 group an intramolecular $\text{N}\cdots\text{H}\cdots\text{O}$ hydrogen bond stabilizes the (ac, sc) structure of the keto tautomer. The intramolecular hydrogen bond is confirmed by the short $r(\text{O2}\cdots\text{H3})$ distances of 2.10(3) Å in MAME, 2.02(3) Å in MA and 2.21(7) Å in AAA. The refined geometrical parameters of MAME can be compared with those of the symmetrically substituted β -diketones malonamide, $\text{NH}_2\text{C}(\text{O})\text{--CH}_2\text{--C}(\text{O})\text{NH}_2$ (MA),⁴ and dimethyl malonate, $\text{H}_3\text{COC}(\text{O})\text{--CH}_2\text{--C}(\text{O})\text{OCH}_3$ (DMM),¹⁶ which have been investigated previously. In MAME, bond lengths and angles in the $\text{NH}_2\text{C}(\text{O})\text{--CH}_2\text{--}$ entity are very similar to those in MA, and the geometry of the $\text{--CH}_2\text{--C}(\text{O})\text{OCH}_3$ entity is again very close to that of DMM. Torsional angles $\tau(\text{C3C1C2O1})$ and $\tau(\text{C2C1C3O2})$ in MAME (140(3)° and 31(7)°, respectively) are close to those in MA (140(4)° and 49(3)°, respectively) but different from those in DMM. Also, these torsional angles in the keto tautomer of AAA³ are close to the values in MAME.

An interesting point in the MAME structure is the problem of planarity of the --NH_2 group. GED cannot answer this question because the torsional angles which characterize the orientation of the N–H bonds cannot be determined reliably. All quantum chemical calculations at different levels of theory predict an almost planar configuration of the --NH_2 group. The experimental N–C2 bond length (1.360(4)Å) is between the values for N–C single bonds (e.g., $r(\text{N–C}) = 1.458(4)$ Å in trimethylamine²¹) and N=C double bonds (e.g., $r(\text{N=C}) = 1.273(4)$ Å in methanimine²²). This demonstrates the presence of strong conjugation between the nitrogen lone pair and π^*

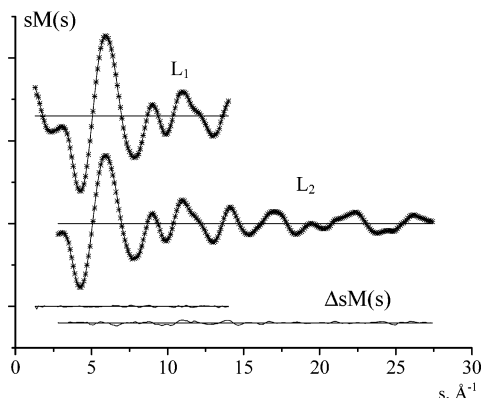


Figure 4. Experimental (dots) and calculated (solid lines) modified molecular intensity curves and residuals (experimental–theoretical) at two nozzle-to-plate distances ($L_1 = 598$ mm, $L_2 = 338$ mm).

orbital of the C=O bond. Delocalization of the lone pair leads to almost planar arrangement of the bonds around nitrogen.

Experimental Section

A commercial sample was used. The electron diffraction patterns and the mass spectra were recorded simultaneously using the techniques described previously.^{23,24} The conditions of the GED/MS experiment and the relative abundance of the characteristic ions of $C_4H_7NO_3$ are shown in the Tables 4 and 5, respectively.

The temperature of the molybdenum effusion cell was measured with a W/Re-5/20 thermocouple that was calibrated by the melting points of Sn and Al. The wavelength of electrons was determined from diffraction patterns of polycrystalline ZnO. The optical densities were measured by a computer controlled MD-100 microdensitometer.²⁵ The molecular intensities $sM(s)$ were obtained in the s ranges $2.8\text{--}27.4 \text{ \AA}^{-1}$ and $1.3\text{--}14.3 \text{ \AA}^{-1}$ for the short and long nozzle-to-plate distance, respectively [$s = (4\pi/\lambda) \sin \theta/2$, λ is electron wavelength, and θ is scattering angle]. The experimental and theoretical intensities $sM(s)$ are compared in Figure 4.

Acknowledgment. We are grateful for financial support from Deutsche Forschungsgemeinschaft (Grant 436RUS113/69/0-6) and Russian Foundation for Basic Research (Grant N07-03-91561-NNIO_a). N.V.B. is grateful to the Deutsche Akademische Austauschdienst (DAAD) and Russian Ministry of Education and Science for a fellowship of her visit to Germany. We also thank Professor G.V. Girichev for the fruitful discussions and for very valuable comments.

References and Notes

(1) (a) Emsley, J. *Struct. Bonding*; Springer: Berlin, 1984; Vol. 57, p 147. (b) Rappoport, Z., Ed.; *The Chemistry of Enols*; John Wiley & Sons:

Chichester, 1990. (c) Sobczyk, L.; Grabowski, S. J.; Krygowski, T. M. (Interaction between H-bond and Pi-electron delocalization) *Chem. Rev.* **2005**, *105*, 3513–3580.

(2) “sp” corresponds to dihedral angle $\tau(\text{C}-\text{C}-\text{C}=\text{O}) = 0 \pm 30^\circ$; “sc” corresponds to $\tau = 60 \pm 30^\circ$; “ac” corresponds to $\tau = 120 \pm 30^\circ$; and “ap” corresponds to $\tau = 180 \pm 30^\circ$.

(3) Belova, N. V.; Girichev, G. V.; Shlykov, S. A.; Oberhammer, H. *J. Org. Chem.* **2006**, *71*, 5298.

(4) Belova, N. V.; Oberhammer, H.; Girichev, G. V.; Shlykov, S. A. *J. Phys. Chem. A* **2007**, *111*, 2248.

(5) Baughcum, S. L.; Duerst, R. W.; Rowe, W. F. *J. Am. Chem. Soc.* **1981**, *103*, 6296.

(6) Baughcum, S. L.; Smith, Z.; Wilson, E. B.; Duerst, R. W. *J. Am. Chem. Soc.* **1984**, *106*, 2260.

(7) Turner, P.; Baughcum, S. L.; Coy, S. L.; Smith, Z. *J. Am. Chem. Soc.* **1984**, *106*, N 8, 2265.

(8) Lowrey, A. H.; George, C.; D’Antonio, P.; Karle, J. *J. Am. Chem. Soc.* **1971**, *93*, N 24, 6399.

(9) Andreassen, A. L.; Bauer, S. H. *J. Mol. Struct.* **1972**, *12*, 381.

(10) Iijima, K.; Ohnogi, A.; Shibata, S. *J. Mol. Struct.* **1987**, *156*, 111.

(11) Srinivasan, R.; Feenstra, J. S.; Park, S. T.; Xu, S.; Zewail, A. H. *J. Am. Chem. Soc.* **2004**, *126*, 2266.

(12) Giricheva, N. I.; Girichev, G. V.; Lapshina, S. B.; Kuzmina, N. P. *Zh. Strukt. Khimii (Russian)* **2000**, *41*, N1, 58.

(13) Andreassen, A. L.; Zebelmann, D.; Bauer, S. H. *J. Am. Chem. Soc.* **1971**, *93*, N 5, 1148; N 21, 7874.

(14) Jin, A. D.; Mack, H.-G.; Waterfeld, A.; Oberhammer, H. *J. Am. Chem. Soc.* **1991**, *113*.

(15) Mack, H.-G.; Oberhammer, H.; Della Vedova, C. D. *J. Mol. Struct.* **1995**, *346*, 51.

(16) Belova, N. V.; Oberhammer, H.; Girichev, G. V. *J. Mol. Struct.* **2004**, *689*, 255.

(17) Belova, N. V.; Oberhammer, H.; Girichev, G. V. *J. Phys. Chem. A* **2004**, *108*, 3593.

(18) Frisch, M. J.; Trucks, G. W.; Schlegel, H. B.; Scuseria, G. E.; Robb, M. A.; Cheeseman, J. R.; Montgomery, J. A., Jr.; Vreven, T.; Kudin, K. N.; Burant, J. C.; Millam, J. M.; Iyengar, S. S.; Tomasi, J.; Barone, V.; Mennucci, B.; Cossi, M.; Scalmani, G.; Rega, N.; Petersson, G. A.; Nakatsuji, H.; Hada, M.; Ehara, M.; Toyota, K.; Fukuda, R.; Hasegawa, J.; Ishida, M.; Nakajima, T.; Honda, Y.; Kitao, O.; Nakai, H.; Klene, M.; Li, X.; Knox, J. E.; Hratchian, H. P.; Cross, J. B.; Adamo, C.; Jaramillo, J.; Gomperts, R.; Stratmann, R. E.; Yazyev, O.; Austin, A. J.; Cammi, R.; Pomelli, C.; Ochterski, J. W.; Ayala, P. Y.; Morokuma, K.; Voth, G. A.; Salvador, P.; Dannenberg, J. J.; Zakrzewski, V. G.; Dapprich, S.; Daniels, A. D.; Strain, M. C.; Farkas, O.; Malick, D. K.; Rabuck, A. D.; Raghavachari, K.; Foresman, J. B.; Ortiz, J. V.; Cui, Q.; Baboul, A. G.; Clifford, S.; Cioslowski, J.; Stefanov, B. B.; Liu, G.; Liashenko, A.; Piskorz, P.; Komaromi, I.; Martin, R. L.; Fox, D. J.; Keith, T.; Al-Laham, M. A.; Peng, C. Y.; Nanayakkara, A.; Challacombe, M.; Gill, P. M. W.; Johnson, B.; Chen, W.; Wong, M. W.; Gonzalez, C.; Pople, J. A. *Gaussian 03*, Revision B.03; Gaussian, Inc.: Pittsburgh, PA, 2003.

(19) (a) Sipachev, V. A. *J. Mol. Struct.* **2001**, *567–568*, 67. (b) Sipachev, V. A. *J. Mol. Struct.* **1985**, *121*, 143. (c) Sipachev, V. A. In *Advances in Molecular Structure Research*; Hargittai, I., Hargittai, M., Eds.; JAI Press: New York, 1999; Vol. 5, p 263.

(20) Andersen, B.; Seip, H. M.; Strand, T. G.; Stolevik, R. *Acta Chem. Scand.* **1969**, *23*, 3224.

(21) Beagley, B.; Medwid, A. R. *J. Mol. Struct.* **1977**, *38*, 229.

(22) Pearson, R., Jr.; Lovas, F. J. *J. Chem. Phys.* **1977**, *66*, 4149.

(23) Girichev, G. V.; Utkin, A. N.; Revichev, Yu. F. *Prib. Tekh. Eksp. (Russian)* **1984**, N2, 187.

(24) Girichev, G. V.; Shlykov, S. A.; and Revichev, Yu. F. *Prib. Tekh. Eksp. (Russian)* **1986**, N4, 167.

(25) Girichev, E. G.; Zakharov, A. V.; Girichev, G. V.; Bazanov, M. I. *Izv. Vysh. Uchebn. Zaved., Technol. Text. Prom. (Russian)* **2000**, *2*, 142.